Optical-absorption bands by exciton-magnon coupling in quasi-two-dimensional antiferromagnets $(C_nH_{2n+1}NH_3)_2MnCl_4$ ($n=1,2,3$)

Taiju Tsuboi
Faculty of Engineering, Kyoto Sangyo University, Kamigamo, Kita-ku, Kyoto 603, Japan
(Received 25 January 1995)

Absorption spectra of layer-structured $(C_nH_{2n+1}NH_3)_2MnCl_4$ with $n=1$ (abbreviated MAMC), $n=2$ (EAMC), and $n=3$ (PAMC) have been investigated in the uv-to-visible light region at temperatures of 15–300 K. In addition to the single-exciton and double-exciton bands caused by the magnetic interaction, an absorption band whose intensity is given by both the two-dimensional magnetic interaction and lattice vibration was found. A sharp magnon sideband with double peaks was observed in EAMC and PAMC. The peak distance is smaller in EAMC than in PAMC. On the other hand, a single peak was observed in MAMC. It is suggested that the splitting of the magnon sideband is caused by the weak ferromagnetism due to spin canting in the layer. The line shape of the magnon sideband is calculated and compared with the observed ones.

I. INTRODUCTION

Crystals $(C_nH_{2n+1}NH_3)_2MnCl_4$ with $n=1$ (abbreviated MAMC), $n=2$ (EAMC), and $n=3$ (PAMC) are orthorhombic with a much larger lattice constant b than the other lattice constants a and c [e.g., $a=7.29$ Å, $b=25.94$ Å, and $c=7.51$ Å for PAMC (Ref. 1)] at room temperature. Reflecting the perovskite-type layer crystal structure, the interlayer Mn^{2+} exchange interaction is considerably weaker than the intralayer exchange interaction.[2,3] Thus these crystals form good examples of two-dimensional (2D) magnetic systems, i.e., Heisenberg antiferromagnets just as Rb_2MnCl_4. The Néel temperature T_N is 43.8, 42.1, and 39.3 K in MAMC, EAMC, and PAMC, respectively.[4]

Intense electric-dipole-allowed magnon sidebands appear in the absorption spectra of magnetic insulators.[5] The magnon sidebands appear in the absorption spectra of magnetic insulators.[5] The magnon sideband arises from the coupling of magnon to exciton. The sideband has a sharp high-energy cutoff and a long low-energy tail as observed in a 3D antiferromagnet MnF_2.[6,7] In the 2D EAMC crystal, a sharp magnon sideband was observed at the low-energy of the Mn^{2+} absorption band associated with the ${}^6A_{1g}\rightarrow{}^4T_{2g}({}^4D)$.[8–10] Unlike the sidebands of 3D magnetic insulators, the sideband has an anomalous shape with cutoffs at both the low- and high-energy sides and with double peaks. It has not been clarified (1) whether such an anomalous shape reflects the 2D magnetism and (2) whether the double peaks appear also in the isomorphous MAMC and PAMC crystals.

The parity-forbidden $d\rightarrow d$ absorption bands have been observed in various transition-metal magnetic insulators. They are caused by either magnetic interaction or lattice vibration. The influence of the magnetic interaction appears in the spin-forbidden bands, while the influence of the lattice vibration appears in the spin-allowed bands.[11–13] In the former magnetic-interaction-induced bands, the integrated intensity becomes a maximum at around T_N in 3D magnets and at around $1.5-2T_N$ in 2D magnets, and it is almost constant at high temperatures, while in the latter lattice-vibration-induced bands, it increases linearly with temperature at high temperatures. Nobody has found clearly another type of absorption band which is caused by both the magnetic interaction and lattice vibration. It is interesting to find such a band, since its appearance is expected theoretically.

Contrary to the 2D antiferromagnets like Rb_2MnCl_4, Rb_2CrCl_4, and $BaMnF_4$, there are few reports on the absorption spectra of $(C_nH_{2n+1}NH_3)_2MnCl_4$ except the reports by Kojima, Ban, and Tsujikawa on two bands in EAMC and PAMC.[8–10] Here we investigate the absorption spectra of MAMC, EAMC, and PAMC in a visible-to-UV light region to try to find the magnetic-interaction-induced and lattice-vibration-induced band and additionally to clarify the similarity and difference in the magnon sidebands among these crystals. For a comparison, we also investigate the absorption spectra of Rb_2MnCl_4 which has the same 2D antiferromagnetism and a similar crystal structure as MAMC, EAMC, and PAMC at room temperature.[14]

II. EXPERIMENTAL PROCEDURE AND RESULTS

Single crystals of $(C_nH_{2n+1}NH_3)_2MnCl_4$ ($n=1,2,3$) were grown by mixing $MnCl_2$ and $CH_2(CH_2)_{n-1}NH_2HCl$ (the ratio is 1:2) in water after melting these materials in HCl liquid at 50 °C. Absorption spectra were measured using a Shimadzu spectrophotometer UV-3100. In the measurement the direction of the incident light was chosen to be parallel to the b axis, i.e., perpendicular to the ac plane. The crystal temperature was changed in a region from 300 to 15 K.

Figure 1 shows the unpolarized absorption spectra of MAMC, EAMC, and PAMC crystals at 15 K. The whole spectra of these crystals is similar to each other and also similar to that of Rb_2MnCl_4.[15,16] Ten absorp-

tion bands (named A, A', B, B', C, D, E, F, G, and α bands in order of increasing energy as indicated in Fig. 1) are observed at the longer wavelength side of 240 nm. The A, A', B, B', C, D, E, F, G, and α bands are located around 530, 505, 460, 436, 417, 370, 355, 335, 270, and 250 nm. Unlike MAMC and EAMC, the α band of PAMC is considerably weak. The C, D, E, and F bands consist of several sharp lines.

The B and G bands have a fine structure with an equidistant progression. The distance is the same between the two bands and it is 212, 208, and 200 cm^{-1} for MAMC, EAMC, and PAMC, respectively. Similar fine structure has been observed in the B band in Rb_2MnCl_4.[16] The frequency of the progression is 240 cm^{-1}. This value has been understood to be the frequency of the A_{1g}-mode lattice vibration coupled to the $^4T_{2g}(^4G)$ excited state.[16] The progression frequencies in MAMC, EAMC, and PAMC are close to each other and near the A_{1g}-mode frequency of Rb_2MnCl_4.

All the bands of $A-F$ in these crystals exhibit a similar temperature dependence to the absorption intensity. A typical behavior is shown in the middle part of Fig. 2 for the F band of PAMC. As temperature is increased from 15 K, the integrated intensity increases until approaching about 80 K, decreases from 85–90 K, stops the decrease at approximately 100 K, and no change above 110 K. This result is consistent with the previous observation[10] on the C band of EAMC and PAMC.

Similarly the G bands show the same temperature dependence in the three crystals, but it is different from the cases of the $A-F$ bands. An example is shown in the upper part of Fig. 2 for the G band in PAMC. The behavior is similar to those of the $A-F$ bands up to about 120 K, but the intensity increases linearly with temperature at high temperatures. Unlike the $A-G$ bands, the intensity of the α band never increases but decreases with increasing temperature from 15 K. The temperature dependence is shown in the lower part of Fig. 2 for the α band on EAMC. As shown in the figure, the intensity is almost constant at the 15–30 K region, decreases quickly until temperature is increased up to about 80 K, and then gradually decreases above 80 K.

A sharp and narrow absorption band (called D_1) is ob-

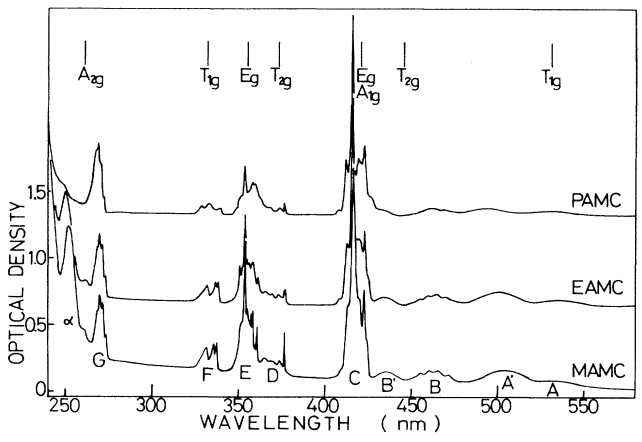

FIG. 1. Unpolarized absorption spectra of $(C_nH_{2n+1}NH_3)_2MnCl_4$ crystals with $n=1$ (MAMC), $n=2$ (EAMC), and $n=3$ (PAMC) at 15 K. The optical density scale for MAMC is shown at the left spindle, while the scale for EAMC and PAMC is not shown. The vertical lines at the upper part indicate the excited energy-level positions of the Mn^{2+} ion in a cubic crystal field.

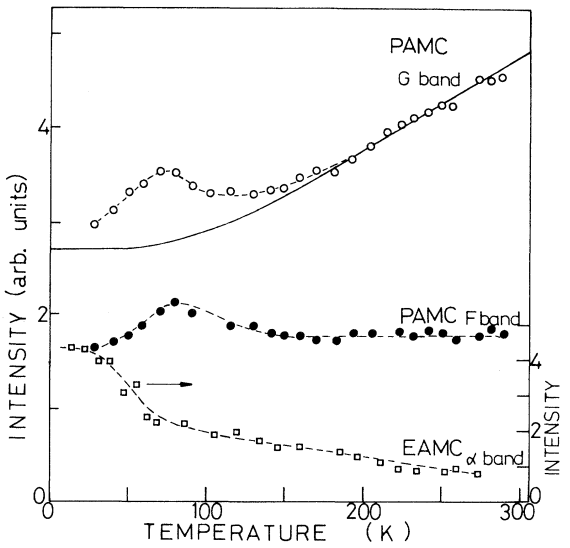

FIG. 2. Temperature dependence of the integrated intensity (i.e., band area) for the G absorption band in PAMC (shown at the upper part of the figure), for the F band in PAMC (the middle part), and for the α band in EAMC (the bottom part). The broken curves are guides to the eye.

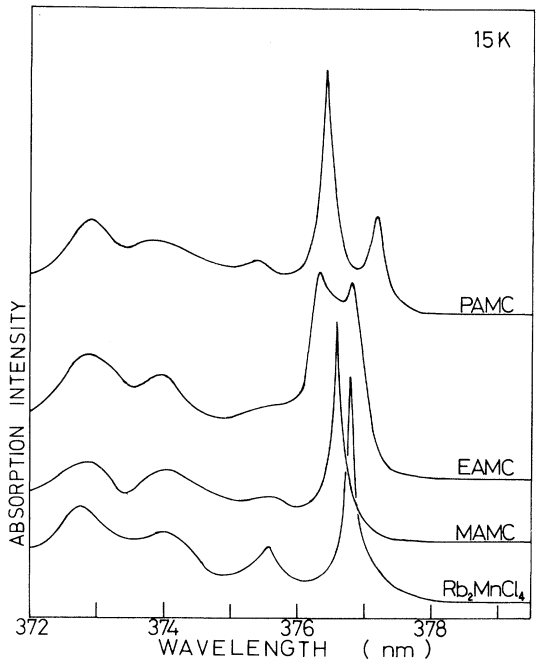

FIG. 3. Absorption spectra of the low-energy side of the D band in MAMC, EAMC, PAMC, and Rb_2MnCl_4 at 15 K.

served at the lowest energy side of the D band in MAMC at low temperatures. The line shape is shown in Fig. 3. The peak position of the D_1 band is located at 376.53 nm at 15 K. Its line shape is asymmetric with a cutoff at the high-energy side. Quite similar line shape is observed for the same D_1 band in Rb_2MnCl_4 as shown in Fig. 3. Such a sharp band is also observed in the D band of EAMC and PAMC. However, the D_1 band of EAMC and PAMC consists of two bands as shown in the upper part of Fig. 3. The energy distance of the two lines is 34 cm^{-1} in EAMC and 55 cm^{-1} in PAMC at 15 K. The two lines approach each other and merge into a single peak with increasing temperature.

III. DISCUSSION

A. Magnetic-interaction- and lattice-vibration-induced bands

Ghosh and Mukherjee calculated an energy-level diagram for Mn^{2+} ion in a cubic crystal field and made level assignments for the absorption bands observed in Rb_2MnCl_4.[15] The positions of the energy levels are shown by vertical lines at the upper part of Fig. 1. Using this energy-level diagram, it is suggested that the A and A' bands are attributable to the transition from the ${}^6A_{1g}$ ground level to the ${}^4T_{1g}(G)$, while the B and B' bands are attributable to the single-exciton bands due to the transition to the ${}^4T_{2g}(G)$ levels. The presence of the two bands in each transition is due to a splitting of these levels by a crystal field with low symmetry such as orthorhombic one. Similarly the C, D, E, F, and G bands are attributable to the single-exciton bands due to the spin- and parity-forbidden transitions from the ${}^6A_{1g}$ level to the ${}^4E_g+{}^4A_{1g}$, ${}^4T_{2g}(D)$, ${}^4E_g(D)$, ${}^4T_{1g}(P)$, and ${}^4A_{2g}$ levels, respectively.

The $A-F$ bands in all the crystals exhibit the same temperature dependence. The intensities of these bands increase with increasing temperature until about $2T_N$ and decrease with further increasing temperature with a maximum intensity at approximately $2T_N$, and no intensity change is observed at temperatures above $3.5T_N$ as shown in Fig. 2. This is characteristic of 2D antiferromagnetism.[10,11] Unlike these absorption bands the G band intensity is not constant at temperatures above 200 K but increases linearly with temperature as shown in Fig. 2.

The intensity of the vibration-induced absorption band is expected to have the following temperature dependence:

$$I(T)=I(0)+I_0\coth(h\nu/2k_BT)\ , \tag{1}$$

where ν is the frequency associated with the lattice vibration.[12,17]

The solid curve of Fig. 2, which is drawn for the G band of PAMC, was obtained using Eq. (1) with the values of $I(0)=1.72$, $I_0=0.223$, and $\nu=200$ cm^{-1}. The $\nu=200$ cm^{-1} value was chosen from the observed progression frequency of the G band, i.e., the frequency of the A_{1g}-mode lattice vibration coupled with the excited state of the G band. The solid curve is found to agree with the observed data at temperatures above 200 K. When the observed intensity is subtracted from the solid curve, we obtain a curve with a maximum at 80–90 K and the temperature dependence is similar to that of the F band shown in the middle of Fig. 2. Therefore it is suggested that the G band intensity is caused by two components: one is the lattice vibration and the other is magnetic interaction. So far temperature dependence obeying Eq. (1) has been observed for the parity- and spin-allowed bands in magnetic insulators, but we observed in the G band that the magnetic interaction is also responsible for the intensity of the spin-forbidden bands. We do not know at this moment why only the G band of many parity- and spin-forbidden bands is influenced by the lattice vibration.

At the high-energy side of the single-exciton bands such as the $A-G$ bands, double-exciton absorption bands have been observed in magnetic insulators.[11,18,19] The double-exciton band is caused by the simultaneous electronic excitation of pairs of nearest-neighbor magnetic ions. Its intensity decreases with increasing temperature. According to the theory,[20] the intensity at high temperature is dropped to 0.32 times of intensity at 0 K. This is consistent with the experimental result of the α band. Therefore the α band is attributed to the double-exciton band. The band is nearly located at the doubled energy of the A' band, indicating that the α band is due to the ${}^6A_{1g}+{}^6A_{1g}\rightarrow{}^4T_{1g}({}^4G)+{}^4T_{1g}({}^4G)$ transition.

The temperature dependence of the double-exciton band intensity is slightly different among the 3D, 2D, and 1D magnets regarding the position of T_N in the temperature dependence curve because the magnetic short-range order is responsible for the intensity.[11,21] The temperature dependence of the double-exciton band intensity observed in 2D antiferromagnet $BaMnF_4$ (Ref. 19) is quite similar to that of the α band in MAMC and EAMC. In this way the 2D antiferromagnetism of MAMC and EAMC is also confirmed from the double-exciton band.

B. Line shape of the magnon sideband

The line shape of the magnon-sideband in 2D antiferromagnets is calculated using the formula which was derived previously.[9] In the derivation were taken into account the exciton dispersion due to the inter- and intrasublattice exciton transfers besides the magnon dispersion. The line shape $u(\nu)$ is expressed as

$$\begin{aligned}u(\nu)\propto\sum_{\mathbf{k}}[&|B|^2\{\sin(ak_x/2)\cos(ak_y/2)\}^2\\&+|C|^2\{\cos(ak_x/2)\sin(ak_y/2)\}^2]\\&\times U_{\mathbf{k}}^2\delta(h\nu-E_{\mathbf{k}}^{\mathrm{ex}}-E_{-\mathbf{k}}^{\mathrm{mag}})\ ,\end{aligned} \tag{2}$$

where B and C are constant, $U_{\mathbf{k}}$ is the coefficient in the transformation which diagonalizes the spin-wave Hamiltonian, and $E_{\mathbf{k}}^{\mathrm{ex}}$ and $E_{-\mathbf{k}}^{\mathrm{mag}}$ mean the exciton and magnon dispersion, respectively.[9] $E_{-\mathbf{k}}^{\mathrm{ex}}$ depends on the matrix elements of inter- and intra-sublattice exciton transfers K_1 and K_2, respectively, while $U_{\mathbf{k}}$ and $E_{\mathbf{k}}^{\mathrm{mag}}$ depend on the nearest-neighbor exchange interaction J_2.[9]

By a parameter fitting, Kojima, Ban, and Tsujikawa obtained a line shape which is quite similar to the observed absorption spectrum of the D_1 band in EAMC. They chose $K_1/|J_1|=\alpha=1.5$ and $K_2/|J_1|=\beta=1.0$ and $|J_1|=6.8$ cm^{-1}. Using the same method, we tried to obtain a line shape which fits the D_1 band observed in each of MAMC and PAMC and also Rb_2MnCl_4 as shown in Fig. 4. A good fit was obtained using values of $\alpha=0.5$ and $\beta=0$ for MAMC and Rb_2MnCl_4, $\alpha=2.0$ and $\beta=1.0$ for PAMC, and $B=1$ and $C=0$ for all the crystals. In our calculation, we used $|J_1|=6.95$, 6.18, and 8.62 cm^{-1} for MAMC, PAMC,[3] and Rb_2MnCl_4,[2] respectively.

The calculated line shape does not agree better with the observed $T=15$ K spectrum of PAMC than the cases of MAMC and Rb_2MnCl_4, although the presence of double peaks and its distance agree with the experiment. If we would take into account the temperature dependence in the calculation, we could obtain a satisfactory agreement. In the near future we will try such a calculation.

The separation of the double peaks is 55 cm^{-1} in PAMC and 34 cm^{-1} in EAMC, while 0 cm^{-1} in MAMC. Why does the splitting of the D_1 band decrease with changing from PAMC to EAMC to MAMC? It is noted that the value of the lattice constant b strongly depends on crystal, i.e., 25.94, 22.09, and 19.4 Å in PAMC,[1] EAMC,[9] and MAMC,[22] respectively, at room temperature. On the other hand, the lattice constants a and c do not exhibit so large a change among these crystals. The splitting in the D_1 band is observed to become wide as the layer separation increases. Therefore it is suggested that the layer separation is responsible for the splitting. This suggestion is not unreasonable since, in the 2D antiferromagnet Rb_2MnCl_4 with $b=16.14$ å,[23] which is near the b value of MAMC, no splitting is observed and the D_1 band shape is quite similar to that of MAMC. Since the 2D magnetic interaction between Mn^{2+} ions becomes strong as the layer separation becomes wide, the wider separation of the double peaks seems to reflect the stronger 2D magnetic interaction.

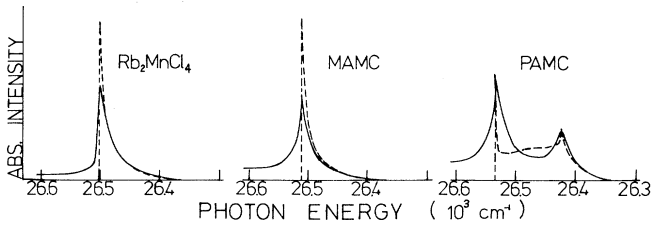

FIG. 4. Comparison of the observed spectrum (solid curve) of the D_1 band in MAMC, PAMC, and Rb_2MnCl_4 at 15 K with a calculated line shape (broken curve).

Nonzero α values were obtained for all of MAMC, EAMC, and PAMC from their D_1 band shapes. This suggests that the intersublattice exciton transfer occurs in these crystals because α is given by $K_1/|J_1|$. This exciton transfer is caused by weak ferromagnetism due to the spin canting.[24] The appearance of the weak ferromagnetism in the layer has been confirmed in these crystals by means of neutron diffraction and superconducting quantum interference device magnetometry.[4] Thus the suggestion derived from the magnon sideband study is consistent with the result of the magnetic study.

ACKNOWLEDGMENTS

The author thanks Professor K. Iio and Dr. T. Kato for providing the crystals which were used in the present work.

[1]E. R. Peterson and R. D. Willet, J. Chem. Phys. **56**, 1879 (1972).
[2]W. van Amstel and L. J. de Jongh, Solid State Commun. **11**, 1423 (1972).
[3]H. A. Groenendijk, A. J. van Duyneveldt, and R. D. Willett, Physica **98B**, 53 (1979).
[4]N. Achiwa, T. Matsuyama, and T. Yoshinari, Phase Transitions **28**, 79 (1990).
[5]Y. Tanabe and K. Aoyagi, *Excitons*, edited by E. I. Rashba and M. D. Sturge (North-Holland, Amsterdam, 1982), p. 603.
[6]D. D. Sell, R. L. Greene, and R. M. White, Phys. Rev. **158**, 489 (1967).
[7]R. S. Meltzer, M. Lowe, and D. S. McClure, Phys. Rev. **180**, 561 (1969).
[8]N. Kojima, T. Ban, and I. Tsujikawa, J. Phys. Soc. Jpn. **41**, 1809 (1976).
[9]N. Kojima, T. Ban, and I. Tsujikawa, J. Phys. Soc. Jpn. **44**, 923 (1978).
[10]N. Kojima, T. Ban, and I. Tsujikawa, J. Phys. Soc. Jpn. **44**, 919 (1978).
[11]T. Tsuboi and W. Kleemann, Phys. Rev. B **27**, 3762 (1983).
[12]T. Tsuboi, M. Chiba, and Y. Ajiro, Phys. Rev. B **32**, 354 (1985).
[13]T. Tsuboi, Phys. Rev. B **32**, 3164 (1985).
[14]B. Schroader, V. Wagner, N. Lehner, K. M. Kesharwani, and R. Geick, Phys. Status Solidi B **97**, 501 (1980).
[15]B. Ghosh and R. K. Mukherjee, Phys. Status Solid B **106**, 699 (1981).
[16]A. Vervoitte, J. C. Canit, B. Briat, and U. Kambli, Phys. Status Solidi B **124**, 87 (1984).
[17]S. Sugano, Y. Tanabe, and H. Kamimura, *Multiplets of Transition-Metal Ions in Crystals* (Academic, New York, 1970).
[18]J. Furguson, Austra. J. Chem. **21**, 307 (1968).
[19]F. J. Schaefer, W. Kleeman, and T. Tsuboi, J. Phys. C **16**, 3987 (1983).
[20]T. Fujiawara, W. Gebhardt, and Y. Tanabe, J. Phys. Soc. Jpn. **33**, 39 (1972).
[21]S. E. Stokowski and D. D. Sell, Phys. Rev. B **3**, 208 (1971).
[22]K. Knorr, I. R. Jahn, and G. Heger, Solid State Commun. **15**, 231 (1974).
[23]E. M. Ali and G. A. Steigmann, Acta Crystallogr. **33**, 2932 (1977).
[24]T. Fujiwara and Y. Tanabe, J. Phys. Soc. Jpn. **37**, 1512 (1974).